Science of the Total Environment 754 (2021) 142144

Contents lists available at ScienceDirect

Science of the Total Environment

journal homepage: www.elsevier.com/locate/scitotenv

Strong biomass burning contribution to ambient aerosol during heating season in a megacity in Northeast China: Effectiveness of agricultural fire bans?

Yuan Cheng [a], Qin-qin Yu [a], Jiu-meng Liu [a,*], Zhen-Yu Du [b], Lin-lin Liang [c], Guan-nan Geng [d], Bo Zheng [e], Wan-li Ma [a], Hong Qi [a], Qiang Zhang [f], Ke-bin He [d]

[a] State Key Laboratory of Urban Water Resource and Environment, School of Environment, Harbin Institute of Technology, Harbin, China
[b] National Research Center for Environmental Analysis and Measurement, Environmental Development Center of the Ministry of Ecology and Environment, Beijing, China
[c] State Key Laboratory of Severe Weather & CMA Key Laboratory of Atmospheric Chemistry, Chinese Academy of Meteorological Sciences, Beijing, China
[d] State Key Joint Laboratory of Environment Simulation and Pollution Control, School of Environment, Tsinghua University, Beijing, China
[e] Laboratoire des Sciences du Climat et de l'Environnement, CEA-CNRS-UVSQ, UMR8212, Gif-sur-Yvette, France
[f] Department of Earth System Science, Tsinghua University, Beijing, China

HIGHLIGHTS

- Haze pollution was investigated during a six-month long heating season in Harbin.
- $PM_{2.5}$ was dominated by OA and its temporal variation tracked that of levoglucosan.
- OA was impacted strongly by agricultural fires with low combustion efficiencies.
- Improving air quality in HC region requires effective control of biomass burning.

GRAPHICAL ABSTRACT

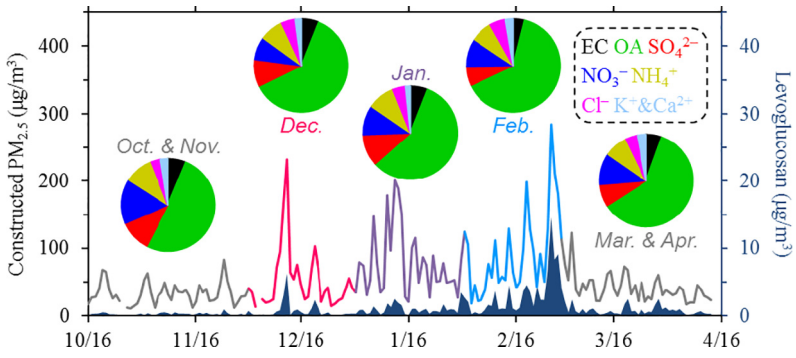

ARTICLE INFO

Article history:
Received 15 May 2020
Received in revised form 28 August 2020
Accepted 31 August 2020
Available online 6 September 2020

Editor: Pingqing Fu

Keywords:
Biomass burning
Organic aerosol
Black carbon
Carbon monoxide
Organic tracer
Agricultural fires

ABSTRACT

Sustainable use of crop residues remains a challenge in main agricultural regions of China such as the Northeast Plain. Here we investigated the impacts of biomass burning on fine particle ($PM_{2.5}$) during a six-month long heating season in the Harbin-Changchun (HC) metropolitan area, China's only national-level city cluster located in the severe cold climate region. Temporal variation of $PM_{2.5}$ was found to coincide with that of levoglucosan. This was attributed to the strong contribution of biomass burning to organic aerosol (the dominant component in $PM_{2.5}$), as supported by the source apportionment results and high levoglucosan-to-organic carbon (OC) ratios. Furthermore, the variation of biomass burning contribution was inferred to be driven mainly by agricultural fires with relatively low combustion efficiencies, based on a synthesis of the relationship between OC and elemental carbon (EC), the dependence of EC on carbon monoxide, and the relative abundances of different tracers for biomass burning. Nitrate formation was enhanced during biomass burning episodes whereas no evidence was observed to indicate enhanced sulfate formation or net increase of OC mass due to secondary formation. This study demonstrates the importance of open burning as a source of haze pollution in the HC region.

* Corresponding author.
E-mail address: jiumengliu@hit.edu.cn (J. Liu).

https://doi.org/10.1016/j.scitotenv.2020.142144
0048-9697/

1. Introduction

Severe haze pollution in China, e.g., that hovering over Beijing for nearly the whole month of January in 2013 (Zheng et al., 2015), has attracted broad attention and led to stringent control measures under the "Air Pollution Prevention and Control Action Plan" promulgated by the State Council of China in September 2013. A nationwide decrease of fine particulate matter ($PM_{2.5}$) occurred with the implementation of the Action Plan, as supported by results from both remote sensing (Wei et al., 2019) and ground-based monitoring network operated by the China National Environmental Monitoring Center (CNEMC; Zhang et al., 2019). Simulations by a chemical transport model suggested that the decrease was mainly driven by reductions in industrial emissions whereas promoting clean fuels in the residential sector also contributed but less significantly (Zhang et al., 2019). It is noteworthy that although residential emissions are caused by the use of both coal and biomass fuels, only the former one is targeted in the Action Plan. More importantly, biomass remains the dominant contributor to primary $PM_{2.5}$ and carbonaceous aerosol in the residential sector (Zhao et al., 2018), despite the decreasing trend in household biomass consumption during the last couple of decades in China (Tao et al., 2018; Zhao et al., 2018). This highlights the benefits of reducing emissions from residential biomass fuels for further improving air quality and protecting public health.

In addition to household use (for cooking and heating), large amounts of biomass are combusted by open burning such as wildfires and agricultural fires, with the latter being a substantial concern in developing counties like China and India (Bikkina et al., 2019). For example, biomass burning (BB) episodes caused by post-harvest burning of crop residues have been repeatedly observed in the North China Plain (Cheng et al., 2013; Yan et al., 2019; Liang et al., 2020), even in recent years under toughest-ever clean air policy. The BB episodes typically exhibited high $PM_{2.5}$ concentrations (e.g., above 200 $\mu g/m^3$ observed at a rural site in Hebei province during the autumn of 2016; Liang et al., 2020), indicating that open burning could temporarily offset or overwhelm the effects of other air pollution control measures. Despite national and local bans on it, open burning is difficult to be eliminated without effective policy towards sustainable use of crop residues, which remains a challenge in China.

The clean air actions implemented in China in recent years are expected to influence not only $PM_{2.5}$ concentration (Zhang et al., 2019) but also its chemical composition. Observational results derived from aerosol mass spectrometer (AMS) measurements during winter in urban Beijing (Hu et al., 2016; Sun et al., 2018; Li et al., 2019a; Xu et al., 2019) showed that the mass concentrations of organic aerosol (OA) were largely comparable during 2010 to 2016 (~30–40 $\mu g/m^3$) and then decreased to ~12 $\mu g/m^3$ in 2017, whereas the contribution of biomass burning OA (BBOA) to total OA was substantially higher for the period of 2014–2017 (~20%) compared to 2010–2013 (~10%). The observed increase in the relative importance of BBOA may be related to the Action Plan, which primarily aimed at reducing fossil fuel emissions. However, such information on aerosol composition is far less comprehensive for other air pollution hotspots in China, making it difficult to properly evaluate the influences of various control measures.

Among the major city clusters in China, the Harbin-Changchun (HC) metropolitan area is unique due to its complex air pollution sources and distinct climate. The HC city cluster is located in the severe cold climate region in Northeast China, where the daily average temperature could be below −20 °C during winter. Thus intensive energy use (e.g., coal and biomass fuels for household space-heating in rural areas) and massive air pollutant emissions are expected during the heating season, which usually lasts as long as six months (i.e., from mid-October through mid-April). In addition, the city cluster is within a main agricultural region in China (i.e., the Northeast Plain; Hou et al., 2019), and open burning of crop residues, although prohibited, has not been completely eliminated in HC and its surrounding areas. Actually, the agricultural fires are not for heating, but they usually take place during the heating season, e.g., after harvesting in autumn or before planting in spring, as indicated by remote sensing studies (Li et al., 2019b; Yin et al., 2019). Anyhow, emissions from biomass burning and other sources have resulted in severe air pollution during heating season in the HC city cluster, with daily and hourly averages of $PM_{2.5}$ reaching as high as ~650 and 1000 $\mu g/m^3$, respectively (Li et al., 2019b).

So far, current understanding of biomass burning impacts on the HC region mainly comes from remote sensing and air quality data (Li et al., 2019b; Yin et al., 2019), whereas very little is known about the linkage between biomass burning emissions and aerosol components. In fact, aerosol composition itself has not been well characterized for HC with limited studies (Li et al., 2020; Ma et al., 2020; Sun et al., 2020). To address this lack of understanding, we conducted field measurements in the central city of the HC metropolitan area (i.e., Harbin), based on daily $PM_{2.5}$ sampling covering the whole heating season. Here we present, for the first time, long-term records of Harbin's $PM_{2.5}$ composition including organic tracers for biomass burning. Our results revealed strong impacts of biomass burning, especially agricultural fires that appeared to have low combustion efficiencies. The relationship between biomass burning emissions and aerosol components also provided insights into the role of BB during haze formation. This study has policy implications regarding the recent rapid energy transitions in China.

2. Methods

Chemical compositions of $PM_{2.5}$ in urban Harbin were measured during a six-month period from 16 October 2018 to 14 April 2019. The sampling was performed on the campus of Harbin Institute of Technology (HIT; 45°45′24″ N, 126°40′49″ E), using a low volume sampler (MiniVol; Airmetrics, OR, USA) operated with pre-baked quartz-fiber filters (2500 QAT-UP; Pall Corporation, NY, USA) at a flow rate of 5 L/min. A total of 180 samples (24-h integrated) were collected. Following the procedures described in Cheng et al. (2013), the samples were analyzed for organic carbon (OC), elemental carbon (EC), levoglucosan (LG), mannosan (MN) and water-soluble inorganic ions. Briefly, OC and EC were measured by a DRI carbon analyzer (Model 2001; Atmoslytic Inc., CA, USA) using the IMPROVE-A temperature protocol with transmittance charring correction. The organic tracers for biomass burning, i.e., LG and MN, were detected by a Dionex ion chromatography (IC) system (ICS-5000$^+$; Thermo Fisher Scientific Inc., MA, USA) using the high-performance anion-exchange chromatography coupled to pulsed amperometric detection (HPAEC-PAD) method. The IC was also used to quantify the inorganic ions including sulfate (SO_4^{2-}), nitrate (NO_3^-), chloride (Cl^-), ammonium (NH_4^+), potassium (K^+) etc. Constructed $PM_{2.5}$ concentration, i.e., $(PM_{2.5})^*$, was calculated as the sum of OA (determined as 1.6 × OC), EC and water-soluble inorganic ions.

Air quality data (including $PM_{2.5}$, inhalable particle, sulfur dioxide, nitrogen dioxide, ozone and carbon monoxide) and meteorological data (including temperature, relative humidity and pressure) during the measurement period were obtained with a time resolution of 1 h from China's National Urban Air Quality Real Time Publishing Platform (http://106.37.208.233:20035/) and Weather Underground (https://www.wunderground.com/weather/cn/harbin/ZYHB), respectively. Specific humidity, i.e., the mass of water vapor in a unit mass of moist air, was calculated based on the meteorological parameters obtained.

3. Results and discussion

3.1. Evidence for strong biomass burning contribution to Harbin's aerosol

$(PM_{2.5})^*$ agreed in general with the measurement results from nearby CNEMC sites (Fig. 1b), supporting the use of the observational data measured at HIT to investigate the $PM_{2.5}$ pollution in urban Harbin. As shown in Fig. 1a, $(PM_{2.5})^*$ varied by one order of magnitude from ~10

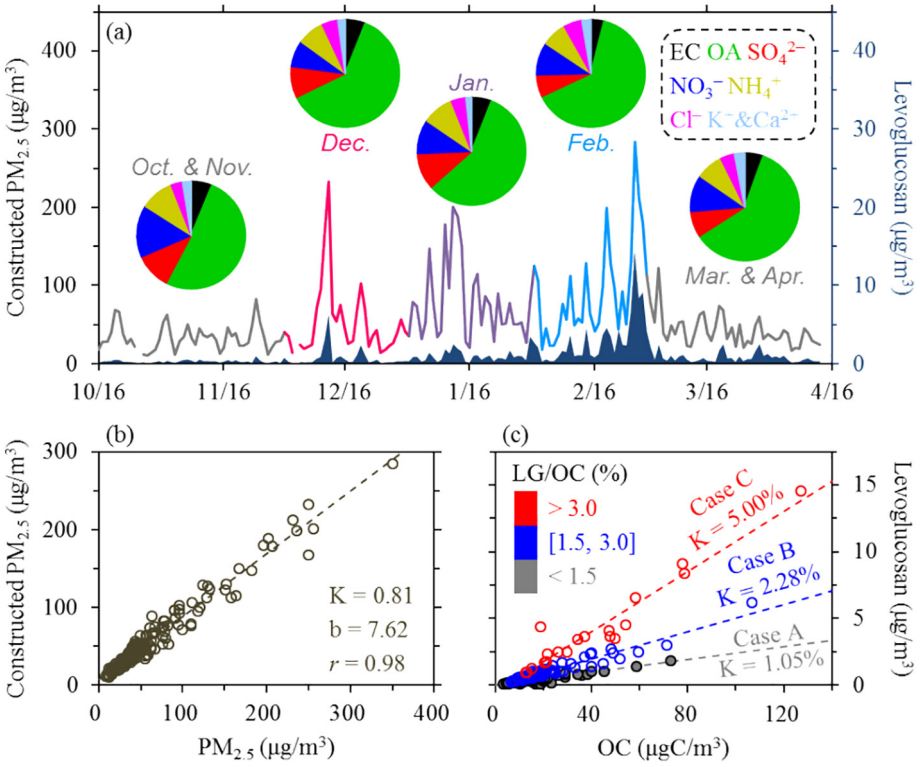

Fig. 1. (a) Temporal variations of constructed $PM_{2.5}$ concentration, i.e., $(PM_{2.5})^*$, and levoglucosan. Monthly average $(PM_{2.5})^*$ compositions are shown by the inner pie charts. (b) Comparison of $(PM_{2.5})^*$ with $PM_{2.5}$ measured at a nearby CNEMC site (45°46′31″ N, 126°41′42″ E; about 2.4 km north of the HIT site). Similar relationship was observed when comparing $(PM_{2.5})^*$ with results from another nearby CNEMC site (45°44′03″ N, 126°41′29″E; about 2.6 km south of the HIT site; not shown here). (C) Relationship between levoglucosan (LG) and OC. Samples are classified into three groups based on the LG/OC ratios. There are 82, 61 and 19 samples in Cases A, B and C, respectively. Dashed lines in (b) and (c) indicate linear regression results, with K and b denoting the slope and intercept, respectively. In (c), the LG/OC ratios and the K (i.e., ΔLG/ΔOC) values are presented on a basis of carbon mass.

to 285 μg/m³ during the measurement period. Furthermore, $(PM_{2.5})^*$ and levoglucosan exhibited similar patterns of temporal variation, e.g., the highest $(PM_{2.5})^*$ and levoglucosan (14.56 μg/m³) were observed in the same sampling event in late February. This pointed to a strong impact of biomass burning on $PM_{2.5}$ throughout the heating season. To better illustrate the role of BB, distinct episodes strongly impacted by dust or firework were excluded in the following discussions. These two types of episodes ($N = 14$ and 2, respectively) were identified by the dependence of $PM_{2.5}$ on inhalable particle (PM_{10}) and the dependence of levoglucosan on K^+, respectively, as described in the Supplementary material (Fig. S1).

Given that BB aerosol mainly consists of carbonaceous species (May et al., 2014), we first investigated the influence of biomass burning on OA, i.e., the dominant component in $(PM_{2.5})^*$ (Fig. 1a). The samples were classified into three groups (namely Cases A, B and C) with LG/OC ranges of <1.5%, between 1.5 and 3.0%, and >3.0% (on a basis of carbon mass), respectively. For the three cases, levoglucosan and OC correlated strongly ($r \geq 0.95$) with slopes, i.e., ΔLG/ΔOC values, of 1.05 ± 0.04, 2.28 ± 0.09 and 5.00 ± 0.34%, respectively (Fig. 1c). The strong correlations between levoglucosan and OC should not be attributed primarily to the influence of meteorological conditions (e.g., wind speed and the planetary boundary layer height), because the correlations between levoglucosan and other components were much weaker (e.g., EC and sulfate; Fig. S2). It could thus be inferred that Fig. 1c pointed to the importance of biomass burning as an OC source for all the three cases. This was supported by the source apportionment results from EPA's Positive Matrix Factorization (PMF) model, i.e., ~50% of OC was attributed to biomass burning for the whole campaign while the BB contributions to OC were estimated to be ~35, 50 and 80% for Cases A, B and C, respectively. Details of the PMF analysis, including the source profiles resolved, are presented in the Supplementary material (SI-1 and Fig. S3).

3.2. Influences of biomass burning on aerosol composition

The three cases exhibited different aerosol concentrations and compositions, for which the changes of biomass burning contribution should be largely responsible. $(PM_{2.5})^*$ exhibited an increasing trend from Cases A through C (Fig. 2a), mainly driven by the increase of OA. For example, if defining excess $(PM_{2.5})^*$ as the increase of the average $(PM_{2.5})^*$ concentration in a more polluted case relative to a less polluted one, OA constituted ~60 and 80% of the excess $(PM_{2.5})^*$ for the Cases B vs. A and the Cases C vs. B comparisons, respectively. Although OA concentration indeed increased from Cases A through C, its contributions to $(PM_{2.5})^*$ were comparable between Cases A and B whereas a considerably higher contribution was observed for Case C (Fig. 2b). For EC and inorganic ions, their contributions to $(PM_{2.5})^*$ were substantially lower in Case C (Fig. 2c and d), with the EC to $(PM_{2.5})^*$ ratio exhibiting an obvious decreasing trend from Cases A through C (Fig. 2c).

3.3. Chemical signatures related to biomass burning

The three cases exhibited different chemical signatures (i.e., ratios between various species), which could be related to the changes of biomass burning contribution as well. First, OC increased more rapidly with increasing EC from Cases A through C. OC and EC correlated strongly ($r = 0.96$) for Case A with a slope (i.e., ΔOC/ΔEC) of 4.04 ± 0.12, whereas for the other cases, the dependences of OC on EC became non-linear and could be approximately by exponential relationships with r values of 0.85 (Fig. 3). Second, linear regression of EC on carbon monoxide (CO) showed lower slopes from Cases A through C, such that the ΔEC/ΔCO values were (5.15 ± 0.31), (4.19 ± 0.37) and $(3.39 \pm 0.57) \times 10^{-3}$ for the three cases, respectively (Fig. 4a). Sampling events that might be subject to wet removal of EC were excluded for the

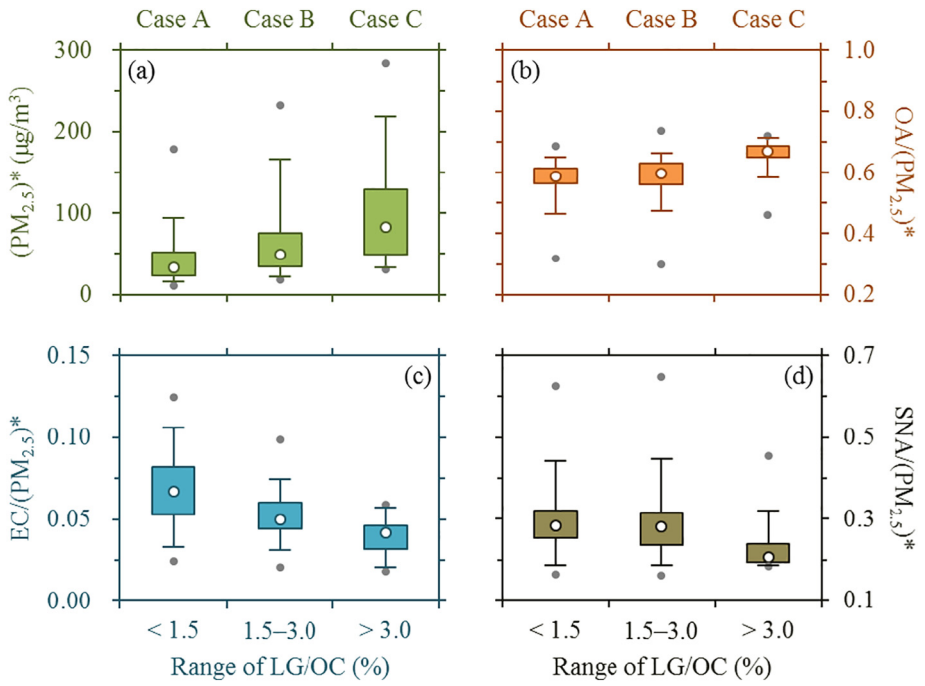

Fig. 2. Comparison of (a) constructed $PM_{2.5}$ concentration, i.e., $(PM_{2.5})^*$, (b) OA to $(PM_{2.5})^*$ ratio, (c) EC to $(PM_{2.5})^*$ ratio, and (d) the sum of sulfate, nitrate and ammonium (SNA) to $(PM_{2.5})^*$ ratio across three cases with different ranges of LG/OC (on a basis of carbon mass). Lower and upper box bounds indicate the 25th and 75th percentiles, the whiskers above and below the box indicate the 95th and 5th percentiles, the solid circles above and below the box indicate the maximum and minimum, and the open circle within the box marks the median.

determination of ΔEC/ΔCO, as described in the Supplementary material (Fig. S4). Third, levoglucosan became more abundant relative to other biomass burning tracers (i.e., mannosan and K^+) from Cases A through C. Although levoglucosan exhibited linear dependences on both mannosan and K^+, different slopes were derived from the three cases. The $\Delta LG/\Delta K^+$ values were 0.61 ± 0.03, 0.98 ± 0.07 and 3.22 ± 0.60 for Cases A, B and C, respectively, and the corresponding ΔLG/ΔMN values were 10.75 ± 0.98, 20.18 ± 2.92 and 35.41 ± 1.31, respectively (Fig. 4b).

Comparing the chemical signatures observed in Harbin's ambient atmosphere with results from biomass burning source emissions suggests

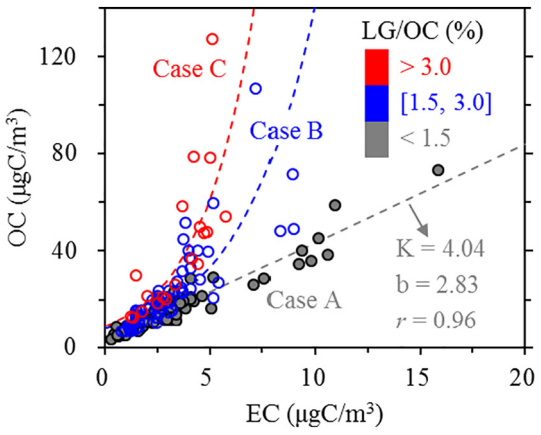

Fig. 3. Dependences of OC on EC for three cases with different ranges of LG/OC (on a basis of carbon mass). The dashed lines indicate regression results. For samples with LG/OC < 1.5% (i.e., Case A), the dependence can be fitted by a linear function with K and b denoting the slope and intercept, respectively. For samples with LG/OC between 1.5 and 3.0% (i.e., Case B), the dependence can be fitted by an exponential function as $OC = 7.85 \times e^{0.29EC}$ ($r = 0.85$). For samples with LG/OC > 3.0% (i.e., Case C), the fitting function is $OC = 8.83 \times e^{0.39EC}$ ($r = 0.85$).

that the influence of smoldering combustion tended to be more significant from Cases A through C. The relative importance of different combustion phases (i.e., flaming and smoldering) to the total emissions during a burn can be estimated by the modified combustion efficiency (MCE), which is calculated based on the molar mixing ratios of CO_2 and CO as $\Delta CO_2/(\Delta CO_2 + \Delta CO)$. In general, higher MCE values indicate a greater contribution from flaming combustion emissions, whereas lower values indicate a greater contribution from smoldering combustion. Laboratory studies such as the Fire Laboratory at Missoula Experiments (FLAME; McMeeking et al., 2009; May et al., 2014) and the Fire Influence on Regional and Global Environments Experiment (FIREX; Selimovic et al., 2019) typically found that little black carbon [BC, referring broadly to results from various measurement principles (Petzold et al., 2013), e.g., EC from thermal-optical method in this study] was emitted at relatively low MCE values (e.g., below 0.9) and in this case, the OC emission factor (EF_{OC}) to EF_{BC} ratio could be as high as ~10^2 whereas the EF_{BC} to EF_{CO} ratio could be as low as ~1.5×10^{-3}. However, EF_{BC} usually increased with increasing MCE and thus at relatively high MCE values (e.g., above 0.95), the EF_{OC} to EF_{BC} ratio could decrease to ~10^{-1} whereas the EF_{BC} to EF_{CO} ratio could increase to ~30×10^{-3}. In laboratory studies, therefore, the EF_{OC} to EF_{BC} ratio was usually found to exhibit a decreasing trend with the increase of MCE whereas an opposite relationship with MCE was typically observed for the EF_{BC} to EF_{CO} ratio. In addition, the dependences of EF_{BC}/EF_{CO} on MCE were found to be comparable between the third FLAME study (i.e., FLAME-III) and a laboratory study conducted in China (Pan et al., 2017), in which the same technique (i.e., the Single Particle Soot Photometer, SP2) was used to measure BC whereas different types of biomass fuels (those commonly seen in the U.S. and China, respectively) were combusted. It seems that in laboratory burns, EF_{BC}/EF_{CO} was influenced mainly by MCE rather than fuel types. The positive dependence of EF_{BC}/EF_{CO} on MCE was also observed in some of the aircraft campaigns focusing on emissions from prescribed fires or wildfires (Kondo et al., 2011; May et al., 2014), although in this case the factors influencing EF_{BC}/EF_{CO} could be more complex than laboratory burns. Anyhow, decrease

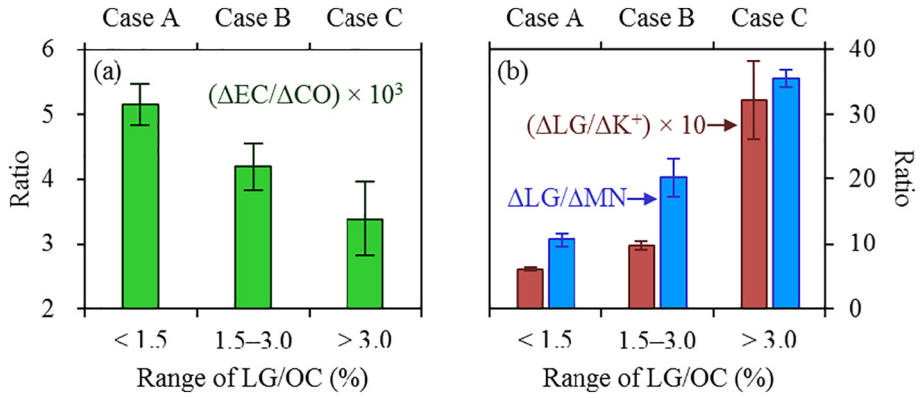

Fig. 4. Comparison of (a) ΔEC/ΔCO and (b) $\Delta LG/\Delta K^+$ and ΔLG/ΔMN across three cases with different ranges of LG/OC (on a basis of carbon mass). The ratios are determined as slopes derived from linear regression.

in EF_{BC}/EF_{CO} and increase in EF_{OC}/EF_{BC} pointed to a greater contribution from smoldering combustion emissions.

Regarding the relative abundances of biomass burning tracers, laboratory studies typically showed larger values of both EF_{LG}/EF_K^+ and EF_{LG}/EF_{MN} at higher EF_{OC}/EF_{BC}. For example, Sullivan et al. (2008) measured BB smoke emitted from the combustion of Manzanita leaves during the first and second FLAME studies (i.e., FLAME-I and -II). The authors found that when EF_{OC}/EF_{BC} increased from 1.2 to 15.0 which were the characteristics of flaming and smoldering combustion, respectively, EF_{LG}/EF_K^+ nearly doubled (from 12.5 to 24.4) while EF_{LG}/EF_{MN} increased from 0.3 to 1.1. Similar trends were observed for other types of biomass fuels (Sullivan et al., 2008). Based on a synthesis of the results from Harbin (Figs. 3 and 4) and BB source emission studies, therefore, it was inferred that the increase of biomass burning contribution from Cases A through C was mainly driven by smoldering combustion emissions.

The chemical signatures also provided information on the types of the biomass fuels that resulted in Harbin's BB aerosols. Based on the source identification method suggested by Cheng et al. (2013), the observed $\Delta LG/\Delta K^+$ and ΔLG/ΔMN values (Fig. 4b) were in general the characteristics of the combustion of crop residues, which typically showed EF_{LG}/EF_K^+ and EF_{LG}/EF_{MN} values of 0.01–1 and 10–100, respectively. Although the relatively high $\Delta LG/\Delta K^+$ in Case C (i.e., above 1) was less commonly seen during laboratory burns of crop residues (Sullivan et al., 2008), comparable values haven been observed in biomass burning episodes caused by post-harvest combustion, e.g., open burning of corn straws during autumn in the North China Plain (Liang et al., 2020).

Given that the occurrences of high LG/OC ratios (e.g., Case C samples) were irregular and no dependence of LG on temperature was observed (Fig. S5), the increase of biomass burning contribution from Cases A through C should be mainly driven by open burning rather than household use of biomass (e.g., for heating and cooking). Furthermore, as indicated by the chemical signatures, the open burning pointed to agricultural fires with relatively low combustion efficiencies.

3.4. Influence of biomass burning on secondary aerosol formation

Sulfate formation was investigated based on the sulfate to EC ratio and the sulfur oxidation ratio (SOR, calculated as the molar ratio of sulfate to the sum of sulfate and sulfur dioxide). Both sulfate/EC and SOR were relatively constant during the study. Their median values observed in different cases were in narrow ranges of 1.6–1.8 and 0.08–0.1, respectively (Fig. 5a and b), showing no evidence that sulfate formation was apparently influenced by biomass burning emissions. Although sulfur dioxide (SO_2) could indeed be detected in BB smoke (Li et al., 2007; Yokelson et al., 2009; Kondo et al., 2011; Liu et al., 2016), results from previous studies did not reach a consensus regarding sulfate formation during atmospheric transport/aging of biomass burning emissions. Sulfate formation was typically slow or even minimal in relatively dry plumes, as observed during the evolution of BB emissions from a chaparral fire in California (Akagi et al., 2012) and for the wildfire plumes transported to the Mt. Bachelor Observatory (MBO) site in Oregon (Collier et al., 2016; Zhou et al., 2017). However, sulfate formation could be fast in BB plumes with relatively high humidity, as observed during the aging of emissions from open fires in Yucatan (Mexico; Yokelson et al., 2009) and Rondônia (Brazil; Morgan et al., 2020). In this study, all the three cases should be considered relatively dry as indicated by both the relative humidity (RH) and specific humidity (C_{water}), e.g., the median RH were ~60, 55 and 40% for Cases A to C, respectively, and the median C_{water} were in a narrow range of $(1.1–1.3) \times 10^{-3}$ (Fig. S6). Given that sulfate formation through photochemistry is much slower than aqueous-phase reactions (in either clouds or aerosol water; Cheng et al., 2016), none of the three cases was favorable for rapid formation of sulfate, despite the increasing trend of ozone concentration from Cases A through C (Fig. S6).

Both nitrate/EC and the nitrogen oxidation ratio (NOR, calculated as the molar ratio of nitrate to the sum of nitrate and nitrogen dioxide) exhibited increasing trends from Cases A through C. The median values of nitrate/EC were 1.1, 1.9 and 2.3 in the three cases, respectively, and the median NOR were 0.05, 0.08 and 0.12, respectively (Fig. 5c and d). This pointed to the influence of biomass burning emissions on nitrate formation. Furthermore, photochemical chemistry should play an important role in this process, as indicated by the increase of ozone with increasing BB contribution and the overall low levels of humidity (Fig. S6). BB-related nitrate formation was also evident in aircraft-based studies focusing on the evolution of biomass burning emissions, e.g., the Studies of Emissions and Atmospheric Composition, Clouds and Climate Coupling by Regional Surveys ($SEAC^4RS$; Liu et al., 2016) campaign and the South American Biomass Burning Analysis (SAMBBA; Morgan et al., 2020) project. Formation of nitrate was typically faster than sulfate in relatively dry BB plumes (Akagi et al., 2012), consistent with the different trends of NOR and SOR observed from Cases A through C in this study.

As discussed in Section 3.3, OC/EC showed an increasing trend from Cases A through C, as the influence of smoldering combustion emissions became more significant. In principle, formation of secondary organic aerosol (SOA) in BB plumes was another likely cause for the observed increase of OC/EC. But this study did not involve robust tracers or indicators for SOA, prohibiting a proper elucidation of BB-related SOA formation. If attributing OC associated with the PMF-based sulfate and nitrate factors (Fig. S3) to secondary OC (SOC), no trend was observed for SOC concentration or the SOC to EC ratio from Cases A through C. The majority of previous field studies also found that OA mass in BB plumes showed little to no change with aging in natural atmosphere (after accounting for dilution; Hodshire et al., 2019), as can be seen

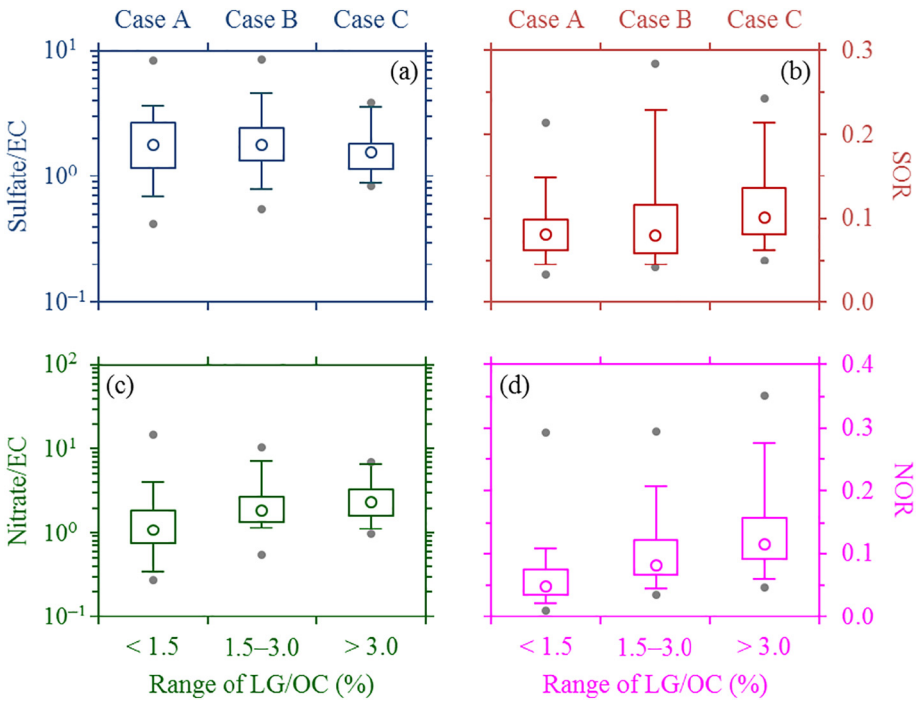

Fig. 5. Comparison of (a) sulfate to EC ratio, (b) SOR, (c) nitrate to EC ratio, and (d) NOR across three cases with different ranges of LG/OC (on a basis of carbon mass).

from ground-based measurements at the MBO site (Collier et al., 2016; Zhou et al., 2017) and aircraft campaigns such as SEAC^{4}RS (Liu et al., 2016), SAMBBA (Morgan et al., 2020) and the Arctic Research of the Composition of the Troposphere from Aircraft and Satellites (ARCTAS; Cubison et al., 2011). However, this does not necessarily mean no evolution of biomass burning OA, because the oxygen to carbon ratios of OA (O/C; retrieved from AMS measurements) were almost always higher in aged plumes than fresh ones (Hodshire et al., 2019). Increase of O/C with aging could be observed even if ΔOA/ΔCO decreased (Forrister et al., 2015; Jolleys et al., 2015). For example, O/C in the Rim plumes nearly doubled in a few hours when ΔOA/ΔCO decreased by ~75% (Forrister et al., 2015). Anyhow, previous studies suggested that complex chemical/physical processes (e.g., formation of SOA and evaporation/decay of primary OA) might be at play during atmospheric aging of biomass burning OA (Jolleys et al., 2012; Hodshire et al., 2019), and the net OA production was usually negligible.

3.5. Conclusions

Haze pollution has not been well understood for the HC metropolitan area, which has not only complex emission sources but also extremely low temperatures during winter (e.g., below −20 °C in terms of daily average). Such atmosphere environment is unique, differing from other air pollution hotspots in China, such as the Beijing-Tianjin-Heibei (also known as Jing-Jin-Ji) region which has been the focus of extensive studies. Based on a six-month field campaign conducted in Harbin (i.e., the central city in HC), here we show that formation of heavily-polluted $PM_{2.5}$ episodes during the heating season was mainly driven by the increase of OC, i.e., the role of secondary inorganic ions was much less important. Furthermore, based on a synthesis of various source-related information such as the PMF results and different chemical signatures, we suggest that biomass burning was the dominant contributor to OC (with an average contribution of ~50%), and its contribution could be considerably enhanced (e.g., ~35 vs. 80% between Cases A and C) by agricultural fires with relatively low combustion efficiencies. However, no evidence was observed to assign the open burning as an important source of EC. A relatively stable biomass burning contribution to EC (~40%) was derived from PMF (Fig. S3), without clear trend from Cases A through C. In addition, formation of nitrate was enhanced during BB episodes (presumably through photochemical reactions) whereas neither enhanced sulfate formation nor net increase of OC mass due to SOA formation was evident.

3.6. Implications

This study revealed distinct influences of biomass burning in the HC region. First, the levoglucosan to OC ratios exceeded 1.5% (on a basis of carbon mass) for ~50% of the Harbin samples. Such high ratios, which are a robust indicator for strong biomass burning impact, are rarely seen in other regions of China (Liu et al., 2019), even during BB episodes caused by open burning (Cheng et al., 2013). Second, the relatively low combustion efficiencies of the agricultural fires impacting Harbin, although not directly measured, appear to differ from the typical open burning conditions in the existing literature (Hodgson et al., 2018). For example, increases in ΔBC/ΔCO were frequently observed during BB episodes in East China (Pan et al., 2011, 2012, 2013), indicating relatively high combustion efficiencies of their open burning conditions. In HC, however, the distinct environment during the heating season, e.g., the low ambient temperature and the snow over the land, may not favor flaming combustion. Given that smoldering combustion promotes PM emission (McMeeking et al., 2009; May et al., 2014), the strong biomass burning impact observed in Harbin should be due not only to the large amounts of crop residues burned but also to the relatively low combustion efficiencies. In future studies, MCE and emission factors of various pollutants should be directly measured for the agricultural fires in the HC region, and transformation of the BB emissions in HC's frigid atmosphere, e.g., formation of secondary organic and inorganic aerosols, should also be investigated.

Regulations of open burning in China rely largely on mandatory bans whereas sustainable use of crop residues remains a difficult challenge. This problem is particularly serious in the HC city cluster which is within a main agricultural region in China. Our results indicate that improvement of air quality cannot be achieved for HC without effective control of open burning.

CRediT authorship contribution statement

Yuan Cheng: Conceptualization, Methodology, Writing - original draft. **Qin-qin Yu:** Investigation. **Jiu-meng Liu:** Conceptualization, Methodology, Writing - original draft. **Zhen-Yu Du:** Investigation. **Lin-lin Liang:** Investigation. **Guan-nan Geng:** Resources. **Bo Zheng:** Resources. **Wan-li Ma:** Resources. **Hong Qi:** Resources. **Qiang Zhang:** Supervision, Writing - review & editing. **Ke-bin He:** Supervision, Writing - review & editing.

Declaration of competing interest

The authors declare that they have no known competing financial interests or personal relationships that could have appeared to influence the work reported in this paper.

Acknowledgments

This work was supported by the National Natural Science Foundation of China (41805097, 4151101089), the Natural Science Foundation of Heilongjiang Province (YQ2019D004), the National Key Research and Development Program (2019YFC0214700), the State Key Laboratory of Urban Water Resource and Environment (2020DX14), the State Key Joint Laboratory of Environment Simulation and Pollution Control (19K02ESPCT), the State Environmental Protection Key Laboratory of Sources and Control of Air Pollution Complex (SCAPC202002) and the Key Laboratory of Atmospheric Chemistry, China Meteorological Administration (2019B04).

Appendix A. Supplementary data

Supplementary data to this article can be found online at https://doi.org/10.1016/j.scitotenv.2020.142144.

References

Akagi, S.K., Craven, J.S., Taylor, J.W., McMeeking, G.R., Yokelson, R.J., Burling, I.R., Urbanski, S.P., Wold, C.E., Seinfeld, J.H., Coe, H., Alvarado, M.J., Weise, D.R., 2012. Evolution of trace gases and particles emitted by a chaparral fire in California. Atmos. Chem. Phys. 12, 1397–1421.

Bikkina, S., Andersson, A., Kirillova, E.N., Holmstrand, H., Tiwari, S., Srivastava, A.K., Bisht, D.S., Gustafsson, Ö., 2019. Air quality in megacity Delhi affected by countryside biomass burning. Nat. Sustain. 2, 200–205.

Cheng, Y., Engling, G., He, K.B., Duan, F.K., Ma, Y.L., Du, Z.Y., Liu, J.M., Zheng, M., Weber, R.J., 2013. Biomass burning contribution to Beijing aerosol. Atmos. Chem. Phys. 13, 7765–7781.

Cheng, Y.F., Zheng, G.J., Wei, C., Mu, Q., Zheng, B., Wang, Z.B., Gao, M., Zhang, Q., He, K.B., Carmichael, G., Pöschl, U., Su, H., 2016. Reactive nitrogen chemistry in aerosol water as a source of sulfate during haze events in China. Sci. Adv. 2, e1601530. https://doi.org/10.1126/sciadv.1601530.

Collier, S., Zhou, S., Onasch, T.B., Jaffe, D.A., Kleinman, L., Sedlacek, A.J., Briggs, N.L., Hee, J., Fortner, E., Shilling, J.E., Worsnop, D., Yokelson, R.J., Parworth, C., Ge, X.L., Xu, J.Z., Butterfield, Z., Chand, D., Dubey, M.K., Pekour, M.S., Springston, S., Zhang, Q., 2016. Regional influence of aerosol emissions from wildfires driven by combustion efficiency: insights from the BBOP campaign. Environ. Sci. Technol. 50, 8613–8622.

Cubison, M.J., Ortega, A.M., Hayes, P.L., Farmer, D.K., Day, D., Lechner, M.J., Brune, W.H., Apel, E., Diskin, G.S., Fisher, J.A., Fuelberg, H.E., Hecobian, A., Knapp, D.J., Mikoviny, T., Riemer, D., Sachse, G.W., Sessions, W., Weber, R.J., Weinheimer, A.J., Wisthaler, A., Jimenez, J.L., 2011. Effects of aging on organic aerosol from open biomass burning smoke in aircraft and laboratory studies. Atmos. Chem. Phys. 11, 12049–12064.

Forrister, H., Liu, J., Scheuer, E., Dibb, J., Ziemba, L., Thornhill, K.L., Anderson, B., Diskin, G., Perring, A.E., Schwarz, J.P., Campuzano-Jost, P., Day, D.A., Palm, B.B., Jimenez, J.L., Nenes, A., Weber, R.J., 2015. Evolution of brown carbon in wildfire plumes. Geophys. Res. Lett. 42, 4623–4630.

Hodgson, A.K., Morgan, W.T., O'Shea, S., Bauguitte, S., Allan, J.D., Darbyshire, E., Flynn, M.J., Liu, D.T., Lee, J., Johnson, B., Haywood, J.M., Longo, K.M., Artaxo, P.E., Coe, H., 2018. Near-field emission profiling of tropical forest and Cerrado fires in Brazil during SAMBBA 2012. Atmos. Chem. Phys. 18, 5619–5638.

Hodshire, A.L., Akherati, A., Alvarado, M.J., Brown-Steiner, B., Jathar, S.H., Jimenez, J.L., Kreidenweis, S.M., Lonsdale, C.R., Onasch, T.B., Ortega, A.M., Pierce, J.R., 2019. Aging effects on biomass burning aerosol mass and composition: a critical review of field and laboratory studies. Environ. Sci. Technol. 53, 10007–10022.

Hou, L.L., Chen, X.G., Kuhn, L.N., Huang, J.K., 2019. The effectiveness of regulations and technologies on sustainable use of crop residue in Northeast China. Energy Econ. 81, 519–527.

Hu, W.W., Hu, M., Hu, W., Jimenez, J.L., Yuan, B., Chen, W.T., Wang, M., Wu, Y.S., Chen, C., Wang, Z.B., Peng, J.F., Zeng, L.M., Shao, M., 2016. Chemical composition, sources, and aging process of submicron aerosols in Beijing: contrast between summer and winter. J. Geophys. Res. Atmos. 121, 1955–1977.

Jolleys, M.D., Coe, H., McFiggans, G., Capes, G., Allan, J.D., Crosier, J., Williams, P.I., Allen, G., Bower, K.N., Jimenez, J.L., Russell, L.M., Grutter, M., Baumgardner, D., 2012. Characterizing the aging of biomass burning organic aerosol by use of mixing ratios: a meta-analysis of four regions. Environ. Sci. Technol. 46, 13093–13102.

Jolleys, M.D., Coe, H., McFiggans, G., Taylor, J.W., O'Shea, S.J., Le Breton, M., Bauguitte, S.J.B., Moller, S., Di Carlo, P., Aruffo, E., Palmer, P.I., Lee, J.D., Percival, C.J., Gallagher, M.W., 2015. Properties and evolution of biomass burning organic aerosol from Canadian boreal forest fires. Atmos. Chem. Phys. 15, 3077–3095.

Kondo, Y., Matsui, H., Moteki, N., Sahu, L., Takegawa, N., Kajino, M., Zhao, Y., Cubison, M.J., Jimenez, J.L., Vay, S., Diskin, G.S., Anderson, B., Wisthaler, A., Mikoviny, T., Fuelberg, H.E., Blake, D.R., Huey, G., Weinheimer, A.J., Knapp, D.J., Brune, W.H., 2011. Emissions of black carbon, organic, and inorganic aerosols from biomass burning in North America and Asia in 2008. J. Geophys. Res. 116, D08204.

Li, X.H., Wang, S.X., Duan, L., Hao, J.M., Li, C., Chen, Y.S., Yang, L., 2007. Particulate and trace gas emissions from open burning of wheat straw and corn stover in China. Environ. Sci. Technol. 41, 6052–6058.

Li, H.Y., Cheng, J., Zhang, Q., Zheng, B., Zhang, Y.X., Zheng, G.J., He, K.B., 2019a. Rapid transition in winter aerosol composition in Beijing from 2014 to 2017: response to clean air actions. Atmos. Chem. Phys. 19, 11485–11499.

Li, Y.C., Liu, J., Han, H., Zhao, T.L., Zhang, X., Zhuang, B.L., Wang, T.J., Chen, H.M., Wu, Y., Li, M.M., 2019b. Collective impacts of biomass burning and synoptic weather on surface $PM_{2.5}$ and CO in Northeast China. Atmos. Environ. 213, 64–80.

Li, N., Wei, X., Han, W.Z., Sun, S.Y., Wu, J.H., 2020. Characteristics and temporal variations of organic and elemental carbon aerosols in PM_1 in Changchun, Northeast China. Environ. Sci. Pollut. Res. 27, 8653–8661.

Liang, L.L., Engling, G., Liu, C., Xu, W.Y., Liu, X.Y., Cheng, Y., Du, Z.Y., Zhang, G., Sun, J.Y., Zhang, X.Y., 2020. Chemical characteristics of $PM_{2.5}$: impact of biomass burning at an agricultural site of the North China Plain during a season of transition. Atmos. Chem. Phys. Discuss. https://doi.org/10.5194/acp-2020-19.

Liu, X.X., Zhang, Y., Huey, L.G., Yokelson, R.J., Wang, Y., Jimenez, J.L., Campuzano-Jost, P., Beyersdorf, A.J., Blake, D.R., Choi, Y., St Clair, J.M., Crounse, J.D., Day, D.A., Diskin, G.S., Fried, A., Hall, S.R., Hanisco, T.F., King, L.E., Meinardi, S., Mikoviny, T., Palm, B.B., Peischl, J., Perring, A.E., Pollack, I.B., Ryerson, T.B., Sachse, G., Schwarz, J.P., Simpson, I.J., Tanner, D.J., Thornhill, K.L., Ullmann, K., Weber, R.J., Wennberg, P.O., Wisthaler, A., Wolfe, G.M., Ziemba, L.D., 2016. Agricultural fires in the southeastern U.S. during SEAC^{4}RS: emissions of trace gases and particles and evolution of ozone, reactive nitrogen, and organic aerosol. J. Geophys. Res. Atmos. 121, 7383–7414.

Liu, X.Y., Zhang, Y.L., Peng, Y.R., Xu, L.L., Zhu, C.M., Cao, F., Zhai, X.Y., Haque, M.M., Yang, C., Chang, Y.H., Huang, T., Xu, Z.F., Bao, M.Y., Zhang, W.Q., Fan, M.Y., Lee, X.H., 2019. Chemical and optical properties of carbonaceous aerosols in Nanjing, eastern China: regionally transported biomass burning contribution. Atmos. Chem. Phys. 19, 11213–11233.

Ma, L.X., Li, B., Liu, Y.P., Sun, X.Z., Fu, D.L., Sun, S.J., Thapa, S., Geng, J.L., Qi, H., Zhang, A.P., Tian, C.G., 2020. Characterization, sources and risk assessment of $PM_{2.5}$-bound polycyclic aromatic hydrocarbons (PAHs) and nitrated PAHs (NPAHs) in Harbin, a cold city in northern China. J. Clean. Prod. 264, 121673.

May, A.A., McMeeking, G.R., Lee, T., Taylor, J.W., Craven, J.S., Burling, I., Sullivan, A.P., Akagi, S., Collett Jr., J.L., Flynn, M., Coe, H., Urbanski, S.P., Seinfeld, J.H., Yokelson, R.J., Kreidenweis, S.M., 2014. Aerosol emissions from prescribed fires in the United States: a synthesis of laboratory and aircraft measurements. J. Geophys. Res. Atmos. 119, 11826–11849.

McMeeking, G.R., Kreidenweis, S.M., Baker, S., Carrico, C.M., Chow, J.C., Collett Jr., J.L., Hao, W.M., Holden, A.S., Kirchstetter, T.W., Malm, W.C., Moosmüller, H., Sullivan, A.P., Wold, C.E., 2009. Emissions of trace gases and aerosols during the open combustion of biomass in the laboratory. J. Geophys. Res. 114, D19210.

Morgan, W.T., Allan, J.D., Bauguitte, S., Darbyshire, E., Flynn, M.J., Lee, J., Liu, D.T., Johnson, B., Haywood, J., Longo, K.M., Artaxo, P.E., Coe, H., 2020. Transformation and aging of biomass burning carbonaceous aerosol over tropical South America from aircraft in-situ measurements during SAMBBA. Atmos. Chem. Phys. 20, 5309–5326.

Pan, X.L., Kanaya, Y., Wang, Z.F., Liu, Y., Pochanart, P., Akimoto, H., Sun, Y.L., Dong, H.B., Li, J., Irie, H., Takigawa, M., 2011. Correlation of black carbon aerosol and carbon monoxide in the high-altitude environment of Mt. Huang in Eastern China. Atmos. Chem. Phys. 11, 9735–9747.

Pan, X.L., Kanaya, Y., Wang, Z.F., Taketani, F., Tanimoto, H., Irie, H., Takashima, H., Inomata, S., 2012. Emission ratio of carbonaceous aerosols observed near crop residual burning sources in a rural area of the Yangtze River Delta Region, China. J. Geophys. Res. 117, D22304.

Pan, X.L., Kanaya, Y., Wang, Z.F., Komazaki, Y., Taketani, F., Akimoto, H., Pochanart, P., 2013. Variations of carbonaceous aerosols from open crop residue burning with transport and its implication to estimate their lifetimes. Atmos. Environ. 74, 301–310.

Pan, X.L., Kanaya, Y., Taketani, F., Miyakawa, T., Inomata, S., Komazaki, Y., Tanimoto, H., Wang, Z., Uno, I., Wang, Z.F., 2017. Emission characteristics of refractory black carbon aerosols from fresh biomass burning: a perspective from laboratory experiments. Atmos. Chem. Phys. 17, 13001–13016.

Petzold, A., Ogren, J.A., Fiebig, M., Laj, P., Li, S.M., Baltensperger, U., Holzer-Popp, T., Kinne, S., Pappalardo, G., Sugimoto, N., Wehrli, C., Wiedensohler, A., Zhang, X.Y., 2013. Recommendations for reporting "black carbon" measurements. Atmos. Chem. Phys. 13, 8365–8379.

Selimovic, V., Yokelson, R.J., McMeeking, G.R., Coefield, S., 2019. In situ measurements of trace gases, PM, and aerosol optical properties during the 2017 NW US wildfire smoke event. Atmos. Chem. Phys. 19, 3905–3926.

Sullivan, A.P., Holden, A.S., Patterson, L.A., McMeeking, G.R., Kreidenweis, S.M., Malm, W.C., Hao, W.M., Wold, C.E., Collett Jr., J.L, 2008. A method for smoke marker measurements and its potential application for determining the contribution of biomass burning from wildfires and prescribed fires to ambient $PM_{2.5}$ organic carbon. J. Geophys. Res. 113, D22302.

Sun, Y.L., Xu, W.Q., Zhang, Q., Jiang, Q., Canonaco, F., Prévôt, A.S.H., Fu, P.Q., Li, J., Jayne, J., Worsnop, D.R., Wang, Z.F., 2018. Source apportionment of organic aerosol from 2-year highly time-resolved measurements by an aerosol chemical speciation monitor in Beijing, China. Atmos. Chem. Phys. 18, 8469–8489.

Sun, X.Z., Wang, K., Li, B., Zong, Z., Shi, X.F., Ma, L.X., Fu, D.L., Thapa, S., Qi, H., Tian, C.G., 2020. Exploring the cause of $PM_{2.5}$ pollution episodes in a cold metropolis in China. J. Clean. Prod. 256, 120275.

Tao, S., Ru, M.Y., Du, W., Zhu, X., Zhong, Q.R., Li, B.G., Shen, G.F., Pan, X.L., Meng, W.J., Chen, Y.L., Shen, H.Z., Lin, N., Su, S., Zhuo, S.J., Huang, T.B., Xu, Y., Yun, X., Liu, J.F., Wang, X.L., Liu, W.X., Cheng, H.F., Zhu, D.Q., 2018. Quantifying the rural residential energy transition in China from 1992 to 2012 through a representative national survey. Nat. Energy 3, 567–573.

Wei, J., Li, Z.Q., Guo, J.P., Sun, L., Huang, W., Xue, W.H., Fan, T.Y., Cribb, M., 2019. Satellite-derived 1-km-resolution PM_1 concentrations from 2014 to 2018 across China. Environ. Sci. Technol. 53, 13265–13274.

Xu, W.Q., Sun, Y.L., Wang, Q.Q., Zhao, J., Wang, J.F., Ge, X.L., Xie, C.H., Zhou, W., Du, W., Li, J., Fu, P.Q., Wang, Z.F., Worsnop, D.R., Coe, H., 2019. Changes in aerosol chemistry from 2014 to 2016 in winter in Beijing: insights from high-resolution aerosol mass spectrometry. J. Geophys. Res. Atmos. 124, 1132–1147.

Yan, C.Q., Sullivan, A.P., Cheng, Y., Zheng, M., Zhang, Y.H., Zhu, T., Collett Jr., J.L., 2019. Characterization of saccharides and associated usage in determining biogenic and biomass burning aerosols in atmospheric fine particulate matter in the North China Plain. Sci. Total Environ. 650, 2939–2950.

Yin, S., Wang, X.F., Zhang, X.R., Zhang, Z.X., Xiao, Y., Tani, H., Sun, Z.Y., 2019. Exploring the effects of crop residue burning on local haze pollution in Northeast China using ground and satellite data. Atmos. Environ. 199, 189–201.

Yokelson, R.J., Crounse, J.D., DeCarlo, P.F., Karl, T., Urbanski, S., Atlas, E., Campos, T., Shinozuka, Y., Kapustin, V., Clarke, A.D., Weinheimer, A., Knapp, D.J., Montzka, D.D., Holloway, J., Weibring, P., Flocke, F., Zheng, W., Toohey, D., Wennberg, P.O., Wiedinmyer, C., Mauldin, L., Fried, A., Richter, D., Walega, J., Jimenez, J.L., Adachi, K., Buseck, P.R., Hall, S.R., Shetter, R., 2009. Emissions from biomass burning in the Yucatan. Atmos. Chem. Phys. 9, 5785–5812.

Zhang, Q., Zheng, Y.X., Tong, D., Shao, M., Wang, S.X., Zhang, Y.H., Xu, X.D., Wang, J.N., He, H., Liu, W.Q., Ding, Y.H., Lei, Y., Li, J.H., Wang, Z.F., Zhang, X.Y., Wang, Y.S., Cheng, J., Liu, Y., Shi, Q.R., Yan, L., Geng, G.N., Hong, C.P., Li, M., Liu, F., Zheng, B., Cao, J.J., Ding, A.J., Gao, J., Fu, Q.Y., Huo, J.T., Liu, B.X., Liu, Z.R., Yang, F.M., He, K.B., Hao, J.M., 2019. Drivers of improved $PM_{2.5}$ air quality in China from 2013 to 2017. Proc. Natl. Acad. Sci. U. S. A. 116, 24463–24469.

Zhao, B., Zheng, H.T., Wang, S.X., Smith, K.R., Lu, X., Aunan, K., Gu, Y., Wang, Y., Ding, D., Xing, J., Fu, X., Yang, X.D., Liou, K.N., Hao, J.M., 2018. Change in household fuels dominates the decrease in $PM_{2.5}$ exposure and premature mortality in China in 2005–2015. Proc. Natl. Acad. Sci. U. S. A. 115, 12401–12406.

Zheng, G.J., Duan, F.K., Su, H., Ma, Y.L., Cheng, Y., Zheng, B., Zhang, Q., Huang, T., Kimoto, T., Chang, D., Pöschl, U., Cheng, Y.F., He, K.B., 2015. Exploring the severe winter haze in Beijing: the impact of synoptic weather, regional transport and heterogeneous reactions. Atmos. Chem. Phys. 15, 2969–2983.

Zhou, S., Collier, S., Jaffe, D.A., Briggs, N.L., Hee, J., Sedlacek, A.J., Kleinman, L., Onasch, T.B., Zhang, Q., 2017. Regional influence of wildfires on aerosol chemistry in the western US and insights into atmospheric aging of biomass burning organic aerosol. Atmos. Chem. Phys. 17, 2477–2493.